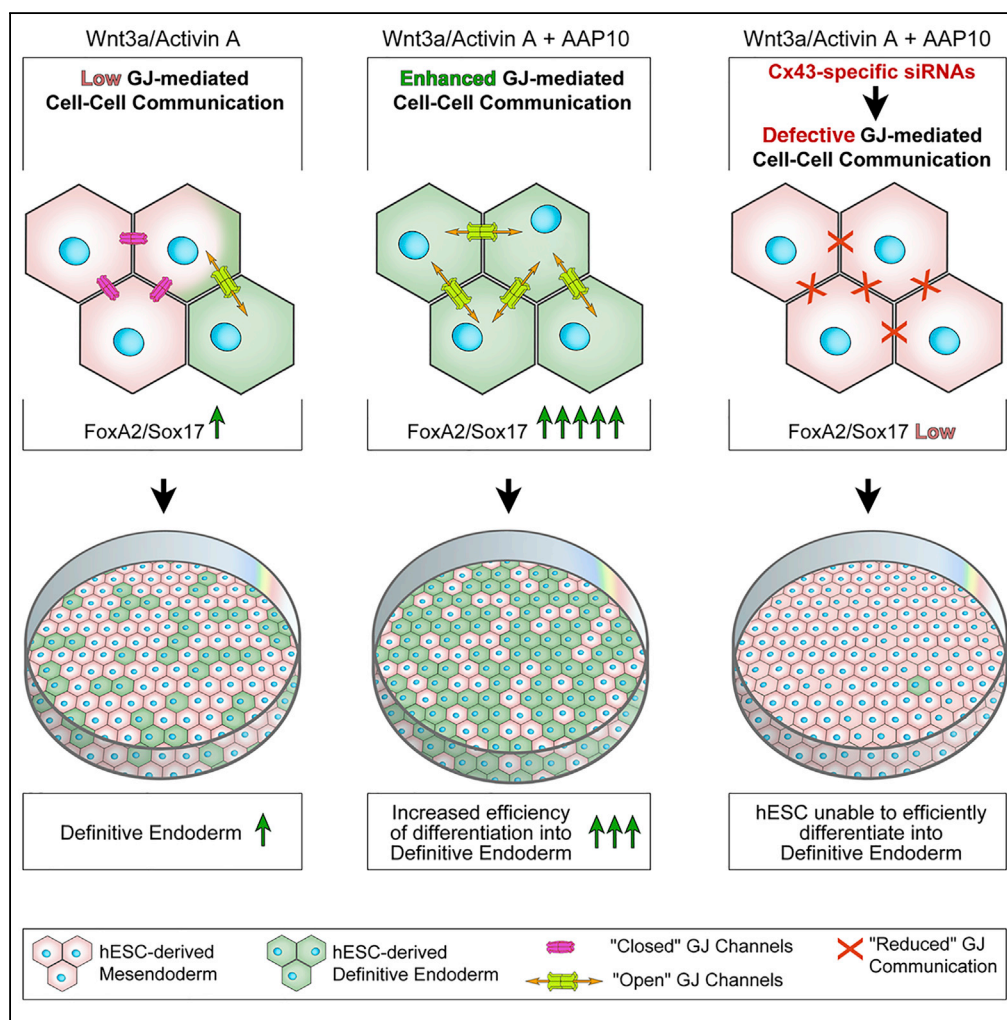**Article**

Connexin 43 Functions as a Positive Regulator of Stem Cell Differentiation into Definitive Endoderm and Pancreatic Progenitors

Wendy Yang, Paul D. Lampe, Patricia Kensel-Hammes, Jennifer Hesson, Carol B. Ware, Laura Crisa, Vincenzo Cirulli

lcrisa@uw.edu (L.C.)
vcirulli@uw.edu (V.C.)

HIGHLIGHTS

Cx43 is upregulated during hESC differentiation into definitive endoderm (DE)

siRNA-mediated knockdown of Cx43 prevents hESC differentiation into DE cells

AAP10-mediated gating of Cx43 gap junctions promotes the expression of FoxA2 and Sox17

Cx43 gap junction communication supports DE and pancreatic progenitors development

Article

Connexin 43 Functions as a Positive Regulator of Stem Cell Differentiation into Definitive Endoderm and Pancreatic Progenitors

Wendy Yang,[1] Paul D. Lampe,[4] Patricia Kensel-Hammes,[1] Jennifer Hesson,[2] Carol B. Ware,[2] Laura Crisa,[1,2,3,]* and Vincenzo Cirulli[1,2,3,5,]*

SUMMARY

Efficient stem cell differentiation into pancreatic islet cells is of critical importance for the development of cell replacement therapies for diabetes. Here, we identify the expression pattern of connexin 43 (Cx43), a gap junction (GJ) channel protein, in human embryonic stem cell (hESC)-derived definitive endoderm (DE) and primitive gut tube cells, representing early lineages for posterior foregut (PF), pancreatic progenitors (PP), pancreatic endocrine progenitors (PE), and islet cells. As the function of GJ channels is dependent on their gating status, we tested the impact of supplementing hESC-derived PP cell cultures with AAP10, a peptide that promotes Cx43 GJ channel opening. We found that this treatment promotes the expression of DE markers FoxA2 and Sox17, leads to a more efficient derivation of DE, and improves the yield of PF, PP, and PE cells. These results demonstrate a functional involvement of GJ channels in the differentiation of embryonic stem cells into pancreatic cell lineages.

INTRODUCTION

The identification of conditions that allows for the *in vitro* differentiation of embryonic stem cells (ESC) and induced pluripotent stem cells (iPSC) toward desired cell lineages have emerged as revolutionary new strategies for the development of cell-based replacement therapies. However, despite significant progress over the past few years, protocols for the induction of these pluripotent stem cells to differentiate into rare cell types, such as the pancreatic islet cells producing hormones like insulin and glucagon, remain relatively inefficient, often leading to heterogeneous cell preparations comprising unwanted cell types that may pose risks of teratoma development following transplantation (Tang et al., 2013; Kushner et al., 2014; Espes et al., 2017).

To date, the majority of protocols for the *in vitro*-directed differentiation of stem cells toward the islet cell lineage have focused on the administration of select growth factors and signaling molecules at defined time points that elicit the activation or inhibition of signaling pathways originally discovered to regulate islet cell development in animal models (Sneddon et al., 2018). In these efforts, one aspect that remains relatively unexplored at the molecular level is the possible role of direct cell-to-cell communication, a mechanism known to regulate cell fate commitment and tissue morphogenesis during development (Constantin and Cronier, 2000; Wei et al., 2004; Levin, 2007; Hatler et al., 2009; Sozen et al., 2014; Yamada et al., 2016). Among proteins that have been shown to participate in these processes of cell communication, connexins (Cxs) are of special interest as they represent the building blocks of gap junction (GJ) channels, mediating the intercellular exchange of signaling molecules such as microRNAs, cations and anions, cyclic nucleotides, as well as small peptides and interfering RNAs (Goodenough et al., 1996; Söhl and Willecke, 2004; Willecke et al., 2002; Evans et al., 2006; Charpantier et al., 2007; Lim et al., 2011; Kanaporis et al., 2008, 2011). These channels have been shown to be indispensable for the proper growth, differentiation, and functional maturation of many cell types, both during embryonic development and in postnatal life (Levin, 2007). Among Cxs known to participate to the biology of pancreatic cell lineages, Cx43 is of particular interest as it is expressed in the developing pancreas where, together with Cx36, it gets progressively restricted to the endocrine cell lineage (Serre-Beinier et al., 2009), and is required for the control of secretory function and survival (Serre-Beinier et al., 2002; Klee et al., 2011; Carvalho et al., 2010, 2012; Nlend et al., 2006; Le Gurun et al., 2003). Interestingly, Cx43 has also been found to be involved in the maintenance of stem cell pluripotency (Dyce et al., 2014), and in the regulation of the cell cycle during tissue

[1]Department of Medicine, UW Diabetes Institute, University of Washington, 850 Republican Street, S475, Seattle, WA 98109, USA

[2]Institute for Stem Cell and Regenerative Medicine, University of Washington, 850 Republican Street, S480, Seattle, WA 98109, USA

[3]Department of Pharmacology, University of Washington, Seattle, WA, USA
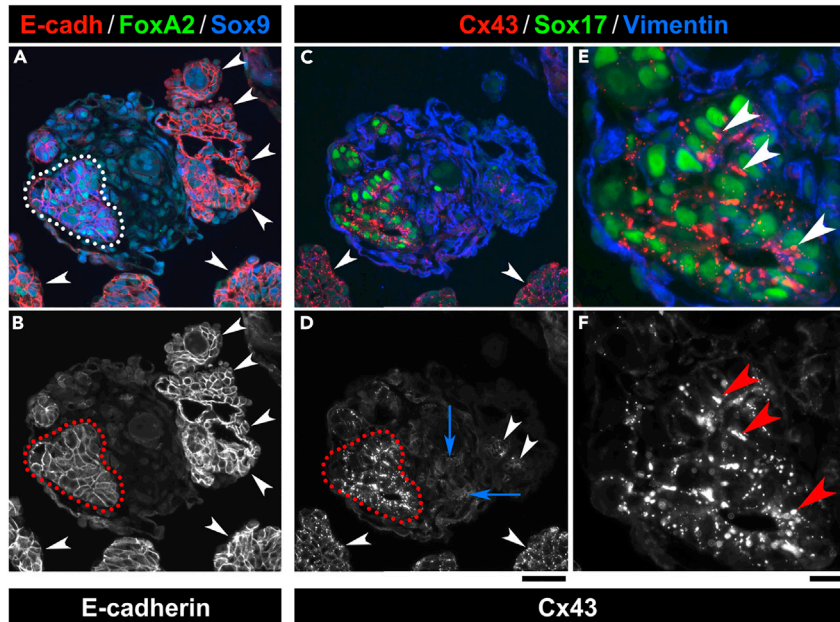
[4]Fred Hutchinson Cancer Research Center, Seattle, WA, USA

[5]Lead Contact

*Correspondence: lcrisa@uw.edu (L.C.), vcirulli@uw.edu (V.C.)

https://doi.org/10.1016/j.isci.2019.07.033

Figure 1. Cx43 Is Preferentially Expressed in Ectoderm and Definitive Endoderm (DE) Developing from hESC In Vitro

(A) Sections of H1 embryoid bodies (EBs) immunostained for E-cadherin (red), FoxA2 (green), and Sox9 (blue), showing areas of E-cadh$^+$FoxA2$^+$Sox9$^+$ definitive endoderm (dotted region), Ecad$^+$FoxA2^{neg}Sox9$^+$ ectoderm (arrowheads), and Ecad^{neg} mesoderm.

(B) Monochromatic image from the microscopic field shown in (A) allows better identification of E-cadherin$^+$ cells.

(C) Serial sections from the same EB preparations immunostained for Cx43 (red), Sox17 (green), and vimentin (blue) reveal that Cx43 is expressed at low levels in ectoderm (arrowheads) and at high levels in Sox17$^+$vimentin^{neg} definitive endoderm cells in the same dotted region defined by the co-expression of E-cadherin, FoxA2, and Sox9 in (A).

(D–F) (E and F) Higher magnification of definitive endoderm cells identified in (C) and (D). Note that immunoreactivity specific for Cx43 is very low in mesoderm cells identified by vimentin expression and lack of E-cadherin immunoreactivity (blue arrows). Images are representative of n = 8 experiments. Scale bars, 50 μm in (A–D) and 20 μm in (E and F).

development and regeneration (Hoptak-Solga et al., 2008). Of further interest are studies demonstrating that interference with Cxs' expression or function results in significant alterations of cell fate development, survival, and differentiated functions (Scherer et al., 2005; Nlend et al., 2006; Wang and Belousov, 2011; Evans et al., 2012).

In this study, building on the notion that the function of GJ channels is dependent on their gating status, we tested a simple gain-of-function approach that promotes the activation or opening of GJ channels composed of Cx43. The approach consisted in treating ESCs undergoing controlled differentiation toward pancreatic cell lineages with the AAP10-activating peptide, reported to promote Cx43 GJ channel opening (Weng et al., 2002; Dhein et al., 2001; Jozwiak and Dhein, 2008; Evans et al., 2012). The results of these experiments demonstrate that activation of Cx43 GJ channels in ESCs significantly enhances the expression of definitive endoderm (DE) markers FoxA2 and Sox17, which in turn results in a more efficient derivation of DE and primitive gut tube (PGT) cells, as well as more prominent numbers of posterior foregut (PF), pancreatic progenitors (PP), and pancreatic endocrine progenitors (EP). Collectively, these results provide evidence for the functional involvement of GJ channels in the differentiation of ESCs into pancreatic cell lineages.

RESULTS

In a first series of experiments, to determine the expression profile of Cx43 in ESCs under conditions that favor spontaneous differentiation, we followed a protocol of suspension culture to generate embryoid bodies (EBs). EB formation recapitulates the early steps of tissue development by yielding lineages with morphological features of ectoderm (ED), mesoderm (MD), and DE (Itskovitz-Eldor et al., 2000; Yirme et al., 2008; Kim et al., 2011). These experiments revealed that DE cells, identified by the co-expression of E-cadherin, Sox9, and Sox17 (Figures 1A–1D, dotted region), exhibited the strongest Cx43-specific
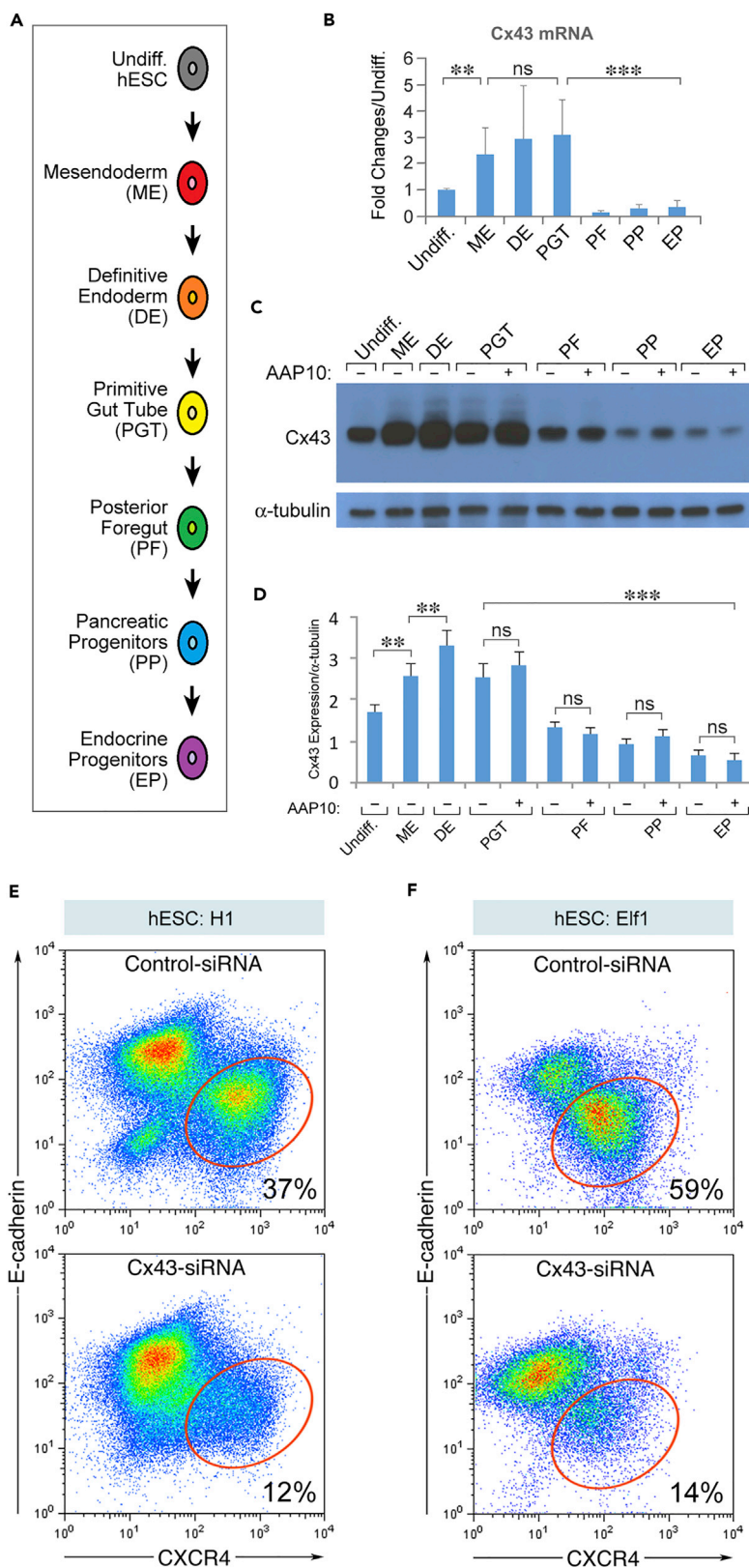
**Figure 2. Expression Profiling of Cx43 in hESC Directed to Differentiate toward Pancreatic Cell Lineages**

(A) Schematic of stepwise protocol for the directed differentiation of hESC into pancreatic cell lineages.

(B) Gene expression of Cx43 throughout all stages of hESC differentiation, as measured by qPCR. Data are presented as mean $\pm$ SD (n = 4). **p < 0.01, ***p < 0.001. Expression of Cx43, although detected in undifferentiated hESC, progressively increases during early stages of differentiation into mesendoderm (ME), definitive endoderm (DE), and primitive gut tube (PGT), followed by a sudden decline after the specification of downstream cell lineages (i.e., posterior foregut [PF]).

(C) Validation of Cx43 protein expression during hESC differentiation, in the presence or absence of AAP10 peptide added at post-DE stages as detected by western blot.

(D) Densitometric analysis of protein bands shown in (C). Bars are mean $\pm$ SE of n = 3 experiments **p < 0.01, ***p < 0.001.

(E and F) (E) Flow cytometric dot plots of DE cells differentiated from H1 and (F) ELF1 hESC lines, as measured by the co-expression of E-cadherin and CXCR4. Knockdown of Cx43 by siRNA results in decreased yield of DE. Representative of n = 3.

immunoreactivity and showed the largest Cx43^{+} junctional plaques (Figures 1E and 1F, arrowheads). ED cells, as defined by the co-expression of E-cadherin and Sox9 (Figures 1A and 1B, arrowheads), also expressed detectable levels of Cx43 (Figures 1C and 1D, arrowheads). In contrast, MD cells, identified by the expression of vimentin and Sox9, and lack of E-cadherin, Sox17, and FoxA2, expressed the lowest levels of CX43 (Figure 1D, blue arrows). From these studies we conclude that during the specification of the three germ layers, the expression of Cx43 segregates with primarily DE and ED cells, with the most prominent levels being expressed in DE cells.

We next investigated the expression profile of Cx43 in ESCs cultured under conditions that direct their differentiation toward the pancreatic cell lineages (D'Amour et al., 2006; Xu et al., 2011; Rezania et al., 2014; Pagliuca et al., 2014; Russ et al., 2015; Nostro et al., 2015; Sambathkumar et al., 2018; Sneddon et al., 2018) (Figure 2A). These studies uncovered a progressive upregulation of Cx43, both at the transcriptional (Figure 2B) and translational levels (Figures 2C and 2D), that peaked at the DE and PGT stages of ESC differentiation, followed by a sudden drop at the posterior foregut (PF) stage. In these experiments, treatment of human ESC (hESC) cultures after the DE stage with the AAP10 peptide, reported to increase Cx43 expression (Easton et al., 2009), had no significant effects on the levels of this GJ protein (Figures 2C and 2D).

Based on these results we hypothesized that Cx43 function is required for proper DE development. Accordingly, in parallel experiments we found that downregulation of Cx43 in two hESC lines, H1 and ELF1 (Ware et al., 2014), by means of Cx43-specific small interfering RNAs (siRNAs) transfected just before the induction of DE differentiation, consistently decreased the yield of Ecad[+]/CXCR4^{+} DE cells, as measured by quantitative flow cytometry (Figures 2E and 2F, % mean $\pm$ SE of DE cell yield in siCx43 cultures = 25% $\pm$ 6% of control siRNA cultures; n = 3). Collectively, these experiments indicate that ESCs undergoing differentiation toward DE rely on the expression of Cx43.

Based on the notion that the function of a given Cx in a cell depends on the gating (opening) of the GJ channels that it forms, we next tested the ability of the AAP10 peptide to elicit GJ-mediated cell-to-cell communication in ESC cultures under conditions of directed differentiation toward pancreatic cell lineages (D'Amour et al., 2006; Xu et al., 2011; Rezania et al., 2014; Pagliuca et al., 2014; Russ et al., 2015; Nostro et al., 2015; Sambathkumar et al., 2018; Sneddon et al., 2018). The rationale for these experiments is based on the demonstration that this peptide has been previously reported to promote Cx43 phosphorylation and GJ channel opening (Weng et al., 2002; Dhein et al., 2001; Jozwiak and Dhein, 2008; Evans et al., 2012), thus providing us with a gain-of-function strategy to determine if a Cx43-mediated increase in cell-cell communication could impact ESC differentiation during early stages of DE induction. As a first step, we tested if the AAP10 peptide was in fact able to enhance cell-cell GJ-mediated communication in our ESC culture conditions. To this end, ESC cultures at the DE stage were supplemented with the AAP10 peptide, and GJ functionality (i.e., opening) was assessed by cell loading of carboxyfluorescein using a scrape-load assay (Opsahl and Rivedal, 2000). These experiments revealed that in control cultures, carboxyfluorescein-loaded cells transferred the fluorescent dye to a few contacting cell layers over a period of 15 min (Figures 3A–3C and 3G). When compared with these controls, cell-cell communication in AAP10-treated cultures was enhanced by ~2 fold, as indicated by the rapid and progressive transfer of the dye from those carboxyfluorescein-loaded cells contacting the wound region to a large number of cells distant from the wound (Figures 3D–3G). In contrast, rhodamine dextran (70 kDa), a dye too large to be transferred through GJ channels, remains confined to the loaded cells at the edge of the wound. Pre-treatment of the cultures with the GJ inhibitor carbenoxolone (Guo et al., 1999) effectively inhibited cell-cell communication
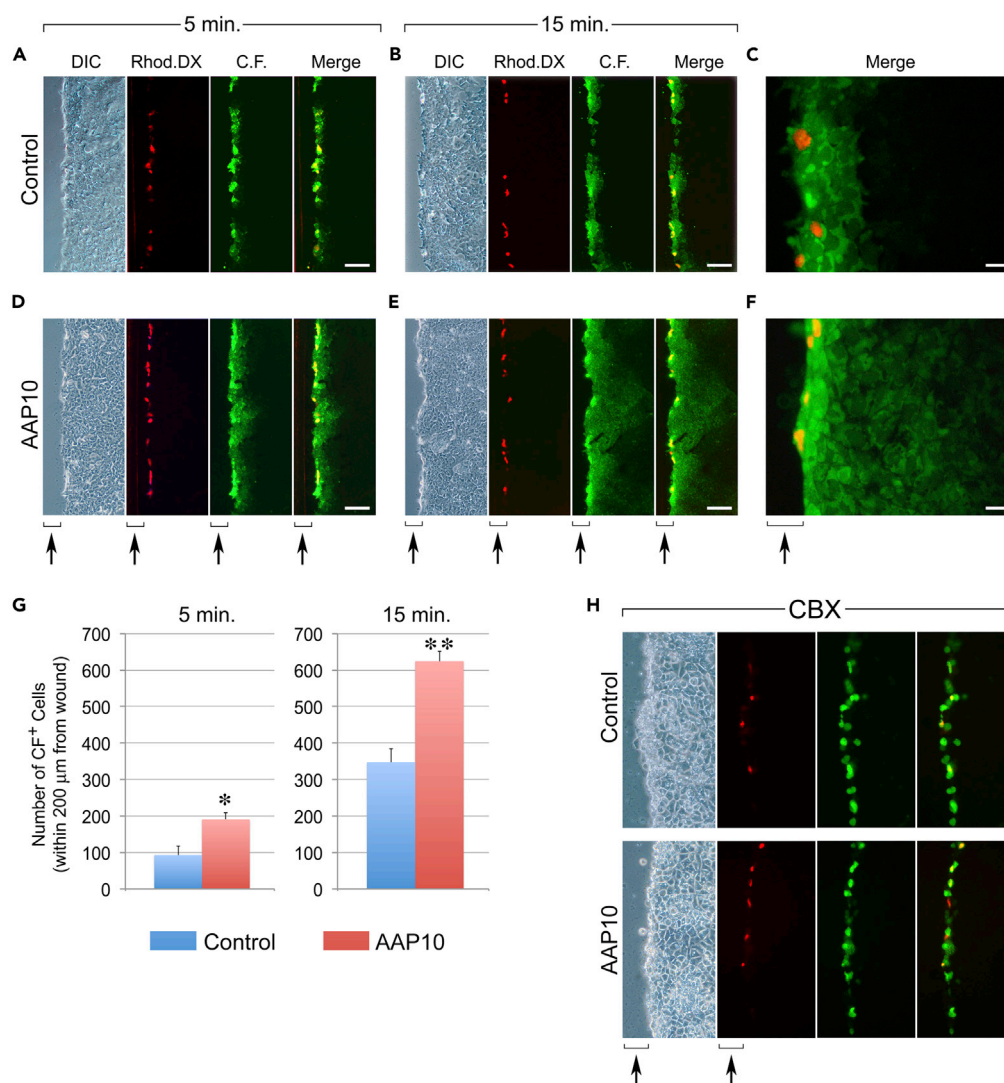
Figure 3. Assessment of GJ Communication in hESC Using a Carboxyfluorescein Scrape-Loading Assay

(A–F) H1 DE monolayers (day 3) were incubated with rhodamine dextran (Rhod DX) and carboxyfluorescein (CF) in the presence or absence of AAP10 (400 nM) and then scraped with a 10-μL pipette tip. After washings, cells at the wound edge (arrows) were imaged by light (DIC) and fluorescent microscopy at 5 (A and D) and 15 min (B, C, E, and F) post-dye loading. Representative of n = 3 independent experiments. Treatment of hESC cultures with the Cx43-activating peptide AAP10 significantly increases CF transfer, indicating enhanced GJ communication. Rhod DX, used as a control, remains confined to the loaded cells at the edge of the wound. Scale bars, 150 μm in (A–E) and 35 μm in (F).

(G) Cumulative quantitative analysis of CF$^+$ cells imaged as in (A–F). Bars are mean $\pm$ SE of CF$^+$ cells counted in 40–50 random areas, on either sides of the wound and up to 200 μm from the wound's edge. *p < 0.05, **p < 0.01.

(H) Imaging of hESC DE cultures pre-treated with carbenoxolone demonstrates effective blockade of CF transfer. Scale bar, 100 μm.

in all cultures (Figure 3H). Collectively, these results demonstrate the efficacy and specificity of AAP10 treatment as a potent activator of GJ communication in differentiating ESCs.

Building on these observations, we next conducted experiments of ESC differentiation in the presence or absence of the AAP10 peptide to determine the impact of Cx43-GJ channel activation on ESC developmental propensity to acquire a DE phenotype. In these studies, we observed that AAP10 treatment results in upregulation of both FoxA2 and Sox17 transcripts (Figure 4A). AAP10 induces a progressive increase of FoxA2-specific transcripts, from ME to DE and PGT stages, followed by a gradual decrease thereafter (Figure 4A, left panel). In contrast, the effect of GJ activation by this peptide on the induction of Sox17-specific
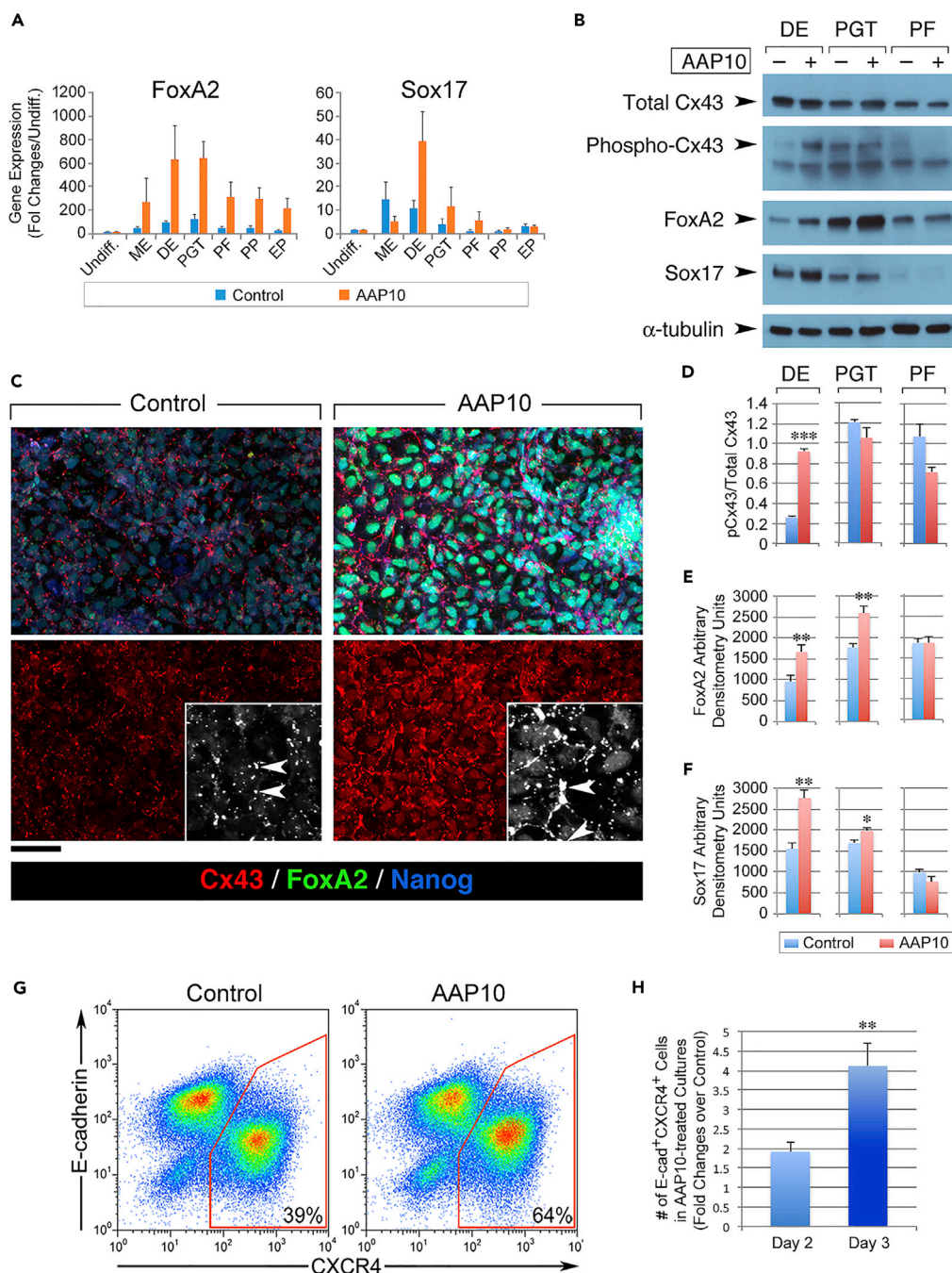
Figure 4. Induction of Definitive Endoderm Is Enhanced by the Cx43 Agonist AAP10 Peptide

(A) qPCR analysis of FoxA2 and Sox17 gene expression in H1 cells throughout all stages of differentiation. Gene expression of these DE markers is increased at DE and PGT stages in cultures treated with AAP10 throughout the differentiation protocol (p < 0.01), followed by a decline during subsequent stages. Bars are mean ± SE of n = 3–4 experiments (no peptide n = 4, AAP10 n = 3).

(B) Western blot analysis of total CX43, phospho-Cx43, FoxA2, and SOX17 protein levels at DE, PGT, and PF stages expressed in cells differentiated in the absence or presence of AAP10 (representative of N = 3).

(C) Immunostaining for Cx43 (red), FoxA2 (green), and Nanog (blue) shows a significant increase in GJ plaque sizes (insets, arrowheads) in H1 DE treated with the AAP10 peptide.

(D–F) Cumulative densitometric analysis of the indicated protein-specific bands detected by western blot shown in (B). Bars are mean ± SD of n = 2–3 experiments. *p < 0.05, **p < 0.01, ***p < 0.001.

Figure 4. Continued

(G) Fluorescence-activated cell sorting analysis of DE cells identified by E-cadherin and CXCR4 co-expression in control and AAP10-treated hESC cultures. Representative of n = 3 experiments.

(H) Cumulative analysis of flow cytometric data as shown in (G), demonstrating increased yield of DE cells generated in the presence of AAP10. N = 4. **p < 0.01.

transcripts occurs more rapidly (within 24 h) from the ME to the DE stage, followed by a rapid decrease at the PGT and subsequent stages of ESC differentiation (Figure 4A, right panel). These results were validated at the protein levels (Figures 4B, 4E, and 4F), indicating that activation of Cx43-GJ channels exerts a potent positive regulatory function on ESC differentiation toward DE and PGT lineages. As part of the same studies we also validated the effects of AAP10 on Cx43 phosphorylation that appears more prominent at the DE stage of ESC differentiation (Figures 4B and 4D). These effects coincided with a notable increase in Cx43-specific immunoreactivity in ESC cultures treated with AAP10 (Figure 4C), which appeared organized into larger GJ plaques in the presence of the peptide (Figure 4C, lower panels, insets, arrowheads). Last, quantitative flow cytometric analysis of DE cultures untreated or treated with AAP10 demonstrated that AAP10-containing cultures yield a higher number of DE cells, as defined by the co-expression of E-cadherin and CXCR4 (Figures 4G and 4H). Together, these results indicate that activation of Cx43-GJ channels during ESC differentiation fosters a more efficient development of DE cell lineages.

Next, to determine if DE cells developing under AAP10 treatment are competent to proceed toward downstream lineages, such as posterior foregut (PF), PP, and EP, we conducted a detailed morphometric analysis for the expression of Pdx1, Nkx6.1, and Sox9, and enumerated cells expressing these markers at each stage of differentiation, in the presence or absence of AAP10. Based on the observed induction of a more efficient DE development when the function of Cx43-GJ channels is activated by AAP10 (Figure 4), we also tested if cell lineages developing downstream of DE and PGT, although expressing significantly lower levels of Cx43, could also benefit from the GJ-activating properties of this peptide. To test this possibility, ESC cultures were differentiated either under control conditions (no peptide treatment), in the presence of AAP10 up to the specification of DE (referred to as "AAP10 Stop @ DE"), or throughout the differentiation process (referred to as "AAP10 Throughout"). These studies revealed that, overall, the development of Pdx1+ progenitors is significantly increased by AAP10 treatment (Figures 5A–5C), although there was no statistical difference between conditions comparing the duration of the AAP10 treatment during the differentiation process (i.e., "AAP10 Stop @ DE" versus "AAP10 Throughout") (Figure 5C). Interestingly, we noted that the frequency of Sox9^{+}Pdx1^{+} (Figures 5A and 5D) and Pdx1^{+}Nkx6.1[+] progenitors (Figures 5B and 5E) was also significantly increased by AAP10 treatment. These results indicate that DE cells produced under conditions that are permissive of Cx43 GJ function have a higher propensity to adopt a differentiation pathway toward PPs and PEs. Together, these studies demonstrate that mechanisms of cell-to-cell communication play an important role in the early specification of development of DE and pancreatic cell lineages from stem cell preparations. Hence, our results may have important implications for the refinement of *in vitro*-directed protocols of stem cells differentiation into pancreatic islet cells.

DISCUSSION

Knowledge gained from the field of developmental biology has played a pivotal role in the design of strategies that have driven our ability to direct the differentiation of stem cells into cell lineages of interest. Despite remarkable progress over the past two decades, a number of limitations remain to be addressed before pluripotent stem cells can be broadly used as a source for the design of cell-based replacement therapies for diseases such as type 1 and possibly type 2 diabetes (D'Amour et al., 2005; D'Amour et al., 2006; Guo et al., 2013; Kroon et al., 2008; Rezania et al., 2011; Rezania et al., 2012). These include the variability between different stem cell lines (both ESCs and iPSCs) with regard to their developmental propensity, or bias, toward one cell lineage versus another; the relative heterogeneity of their differentiated progeny following *in vitro*-directed differentiation; as well as the incomplete functional maturation that would make these cell preparations desirable for clinical applications. Hence, more recent efforts have been devoted to strategies that could minimize some of these concerns (Pagliuca et al., 2014; Rezania et al., 2014; Russ et al., 2015; Zhu et al., 2016).

In the present study we identified an important role of the GJ protein Cx43 as a positive regulator of DE cells from ESCs. We show that the functional activation of Cx43 GJ channels by the AAP10 peptide in ESCs under culture conditions that promote their differentiation results in a robust induction of genes such as FoxA2 and Sox17 (Figure 4), followed by a significant improvement of DE specification. In turn,
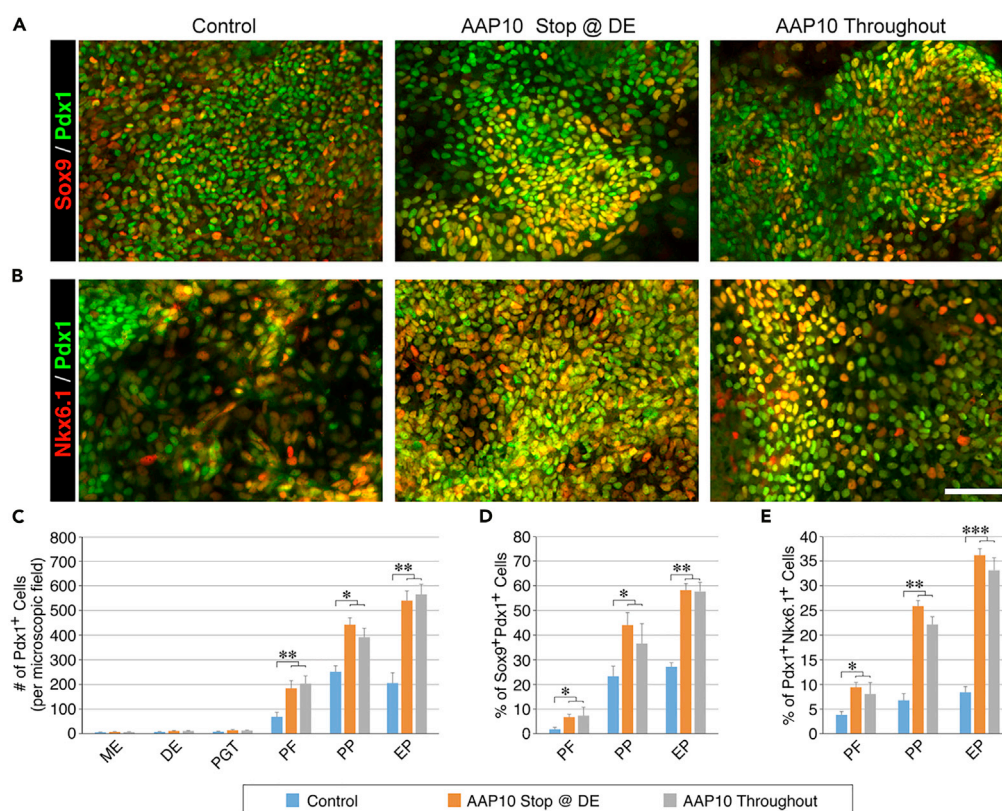
Figure 5. Activation of Cx43 GJ by AAP10 during Early Stages of ESC Differentiation Results in Greater Induction of Pdx1⁺Nkx6.1⁺ Progenitors

(A and B) Immunostaining of ESC cultures at the end of the differentiation protocol (A) for Sox9 (red) and Pdx1 (green) and (B) for Nkx6.1 (red) and Pdx1 (green). Treatment with AAP10 was conducted either up to the DE stage (AAP10 Stop @ DE), or throughout the duration of the differentiation protocol (AAP10 Throughout).

(C) Morphometric assessment of the frequency of Pdx1+ cells in the different culture conditions.

(D and E) Percentage of (D) Sox9⁺Pdx1⁺ cells and (E) Pdx1⁺Nkx6.1⁺ cells in ESC cultures under control and AAP10 treatments. Images shown in (A) and (B) are representative of n = 3. Data presented in (C–E) were from n = 3 independent experiments. $*p < 0.05$; $**p < 0.01$; $***p < 0.001$.

DE cells developing from these cultures proceed with higher efficiency toward PF, PP, and EP cell lineages, as determined by a higher frequency of Sox9⁺Pdx1⁺ and Pdx1⁺Nkx6.1⁺ progenitors (Figure 5).

Although a role of Cx43 in the development and function of pancreatic islets has been previously analyzed in rodent and human pancreas (Charollais et al., 1999; Serre-Beinier et al., 2009; Carvalho et al., 2010), our studies uncover the expression profile and function of this GJ protein during the early induction of DE cells and their downstream differentiation into PPs. Thus, whereas downregulation of Cx43 by RNA interference produced a significant reduction of DE cells developing from ESCs (Figures 2E and 2F), the functional activation of Cx43 by the AAP10 peptide resulted in the induction of FoxA2 and Sox17 genes (Figures 4A–4F), followed by a more efficient differentiation of ESCs into DE cells (Figure 4G). These results suggest that yet-to-be-identified signals exchanged through Cx43 GJ channels between differentiating ESCs must positively affect developmental decisions in ESCs. Our conclusions are also in agreement with those of previous studies showing that the combined genetic ablation of Cx43 and Cx45 in mouse ESC results in their failure to form primitive endoderm representing a key inductive stage for further differentiating into downstream cell lineages (Nishii et al., 2014; Wörsdörfer et al., 2017), while other studies have also suggested an important dynamic modulation of Cx43 during hESC differentiation (Galat et al., 2012; Peng et al., 2019).

The apparent normal development of pancreatic lineages in Cx43 mutant mice (Charollais et al., 1999) might be explained by possible species differences or compensatory functions contributed by other Cxs also expressed in the pancreas (Serre-Beinier et al., 2002, 2009; Carvalho et al., 2010).

Collectively, our results indicate that Cx43 GJ-mediated signaling events are important for a more efficient development of PP and EP cell lineages (Figure 5). Based on previous reports showing that Cx43 function is required for the expansion of the pancreatic islet cell mass (Klee et al., 2011), our findings suggest that the function of this GJ protein may be dynamically regulated at distinct stages of ESC differentiation to encompass regulation of the cell cycle and promote the expansion of select cell lineages. This possibility is supported by the observation that Cx43 has been previously implicated in the regulation of EMT during the generation of human iPSCs (Ke et al., 2013), and in mechanisms mediating the maintenance of stem cell pluripotency (Dyce et al., 2014). Collectively, these results provide significant experimental premise for the future design and identification of agonists that can selectively promote Cx-mediated cell-to-cell communication for a more efficient derivation of pancreatic islet cells.

Limitations of the Study

Our studies took advantage of the validated properties of the AAP10 peptide that has been characterized as a potent activator of Cx43 function and that has been used clinically to promote the synchronization of cardiomyocytes and treat arrhythmias (Weng et al., 2002; Dhein et al., 2001; Jozwiak and Dhein, 2008; Evans et al., 2012). At present, although our results demonstrate an important role of Cx43 GJ function in the differentiation of ESCs into DE cells, and downstream cell lineages, it remains to be determined if enhancing intercellular communication mediated by other Cxs at subsequent stages of ESC differentiation may further improve yields of pancreatic islet cells from cultures of pluripotent stem cells. Based on the inherent difficulty in manipulating these mechanisms of cell communication, future studies will have to focus on the development of appropriate tools that allow the activation of other Cxs. Hence, based on our previous work demonstrating the importance of Cx36 in the development and function of human β-cells (Serre-Beinier et al., 2009), we anticipate that non-genetic gain-of-function approaches like the one used in this study will provide opportunities for testing the impact of activating cell-cell communication during processes of endocrine differentiation and maturation of progenitors into functional islet cells.

METHODS

All methods can be found in the accompanying Transparent Methods supplemental file.

SUPPLEMENTAL INFORMATION

Supplemental Information can be found online at https://doi.org/10.1016/j.isci.2019.07.033.

AUTHOR CONTRIBUTIONS

W.Y., L.C., and V.C. designed, conducted experiments, and analyzed data; C.B,W, P. K.-H., and J.H. provided support for the use of hESC and maintained undifferentiated hESC cultures; P.D.L. provided advice and reagents on the biology of Cx43 and guidance on the project; V.C supervised the project and wrote the manuscript.

DECLARATION OF INTERESTS

The authors declare no competing interests.

iScience

CellPress

REFERENCES

Carvalho, C.P., Barbosa, H.C., Britan, A., Santos-Silva, J.C., Boschero, A.C., Meda, P., and Collares-Buzato, C.B. (2010). Beta cell coupling and connexin expression change during the functional maturation of rat pancreatic islets. Diabetologia *53*, 1428–1437.

Carvalho, C.P., Oliveira, R.B., Britan, A., Santos-Silva, J.C., Boschero, A.C., Meda, P., and Collares-Buzato, C.B. (2012). Impaired β-cell-β-cell coupling mediated by Cx36 gap junctions in prediabetic mice. Am. J. Physiol. Endocrinol. Metab. *303*, E144–E151.

Charollais, A., Serre, V., Mock, C., Cogne, F., Bosco, D., and Meda, P. (1999). Loss of alpha 1 connexin does not alter the prenatal differentiation of pancreatic beta cells and leads to the identification of another islet cell connexin. Dev. Genet. *24*, 13–26.

Charpantier, E., Cancela, J., and Meda, P. (2007). Beta cells preferentially exchange cationic molecules via connexin 36 gap junction channels. Diabetologia *50*, 2332–2341.

Constantin, B., and Cronier, L. (2000). Involvement of gap junctional communication in myogenesis. Int. Rev. Cytol. *196*, 1–65.

D'Amour, K.A., Agulnick, A.D., Eliazer, S., Kelly, O.G., Kroon, E., and Baetge, E.E. (2005). Efficient differentiation of human embryonic stem cells to definitive endoderm. Nat. Biotechnol. *23*, 1534–1541.

D'Amour, K.A., Bang, A.G., Eliazer, S., Kelly, O.G., Agulnick, A.D., Smart, N.G., Moorman, M.A., Kroon, E., Carpenter, M.K., and Baetge, E.E. (2006). Production of pancreatic hormone-expressing endocrine cells from human embryonic stem cells. Nat. Biotechnol. *24*, 1392–1401.

Dhein, S., Weng, S., Grover, R., Tudyka, T., Gottwald, M., Schaefer, T., and Polontchouk, L. (2001). Protein kinase Calpha mediates the effect of antiarrhythmic peptide on gap junction conductance. Cell Commun. Adhes. *8*, 257–264.

Dyce, P.W., Li, D., Barr, K.J., and Kidder, G.M. (2014). Connexin43 is required for the maintenance of multipotency in skin-derived stem cells. Stem Cells Dev. *23*, 1636–1646.

Easton, J.A., Petersen, J.S., and Martin, P.E. (2009). The anti-arrhythmic peptide AAP10 remodels Cx43 and Cx40 expression and function. Naunyn. Schmiedebergs Arch. Pharmacol. *380*, 11–24.

Evans, W.H., Bultynck, G., and Leybaert, L. (2012). Manipulating connexin communication channels: use of peptidomimetics and the translational outputs. J. Membr. Biol. *245*, 437–449.

Espes, D., Lau, J., and Carlsson, P.O. (2017). Mechanisms in Endocrinology: towards the clinical translation of stem cell therapy for type 1 diabetes. Eur. J. Endocrinol. *177*, R159–R168.

Evans, W.H., De Vuyst, E., and Leybaert, L. (2006). The gap junction cellular internet: connexin hemichannels enter the signalling limelight. Biochem. J. *397*, 1–14.

Galat, V., Malchenko, S., Galat, Y., Ishkin, A., Nikolsky, Y., Kosak, S.T., Soares, B.M., Iannaccone, P., Crispino, J.D., and Hendrix, M.J. (2012). A model of early human embryonic stem cell differentiation reveals inter- and intracellular changes on transition to squamous epithelium. Stem Cells Dev. *21*, 1250–1263.

Goodenough, D.A., Goliger, J.A., and Paul, D.L. (1996). Connexins, connexons and intercellular communication. Annu. Rev. Biochem. *65*, 475–502.

Guo, T., Landsman, L., Li, N., and Hebrok, M. (2013). Factors expressed by murine embryonic pancreatic mesenchyme enhance generation of insulin-producing cells from hESCs. Diabetes *62*, 1581–1592.

Guo, Y., Martinez-Williams, C., Gilbert, K.A., and Rannels, D.E. (1999). Inhibition of gap junction communication in alveolar epithelial cells by 18alpha-glycyrrhetinic acid. Am. J. Physiol. *276*, L1018–L1026.

Hatler, J.M., Essner, J.J., and Johnson, R.G. (2009). A gap junction connexin is required in the vertebrate left-right organizer. Dev. Biol. *336*, 183–191.

Hoptak-Solga, A.D., Nielsen, S., Jain, I., Thummel, R., Hyde, D.R., and Iovine, M.K. (2008). Connexin43 (GJA1) is required in the population of dividing cells during fin regeneration. Dev. Biol. *317*, 541–548.

Itskovitz-Eldor, J., Schuldiner, M., Karsenti, D., Eden, A., Yanuka, O., Amit, M., Soreq, H., and Benvenisty, N. (2000). Differentiation of human embryonic stem cells into embryoid bodies comprising the three embryonic germ layers. Mol. Med. *6*, 88–95.

Jozwiak, J., and Dhein, S. (2008). Local effects and mechanisms of antiarrhythmic peptide AAP10 in acute regional myocardial ischemia: electrophysiological and molecular findings. Naunyn. Schmiedebergs. Arch. Pharmacol. *378*, 459–470.

Kanaporis, G., Mese, G., Valiuniene, L., White, T.W., Brink, P.R., and Valiunas, V. (2008). Gap junction channels exhibit connexin-specific permeability to cyclic nucleotides. J. Gen. Physiol. *131*, 293–305.

Kanaporis, G., Brink, P.R., and Valiunas, V. (2011). Gap junction permeability: selectivity for anionic and cationic probes. Am. J. Physiol. Cell Physiol. *300*, C600–C609.

Ke, Q., Li, L., Cai, B., Liu, C., Yang, Y., Gao, Y., Huang, W., Yuan, X., Wang, T., Zhang, Q., et al. (2013). Connexin 43 is involved in the generation of human-induced pluripotent stem cells. Hum. Mol. Genet. *22*, 2221–2233.

Kim, J.M., Moon, S.H., Lee, S.G., Cho, Y.J., Hong, K.S., Lee, J.H., Lee, H.J., and Chung, H.M. (2011). Assessment of differentiation aspects by the morphological classification of embryoid bodies derived from human embryonic stem cells. Stem Cells Dev. *20*, 1925–1935.

Klee, P., Allagnat, F., Pontes, H., Cederroth, M., Charollais, A., Caille, D., Britan, A., Haefliger, J.A., and Meda, P. (2011). Connexins protect mouse pancreatic β cells against apoptosis. J. Clin. Invest. *121*, 4870–4879.

Kroon, E., Martinson, L.A., Kadoya, K., Bang, A.G., Kelly, O.G., Eliazer, S., Young, H., Richardson, M., Smart, N.G., and Cunningham, J. (2008). Pancreatic endoderm derived from human embryonic stem cells generates glucose-responsive insulin-secreting cells in vivo. Nat. Biotechnol. *26*, 443–452.

Kushner, J.A., MacDonald, P.E., and Atkinson, M.A. (2014). Stem cells to insulin secreting cells: two steps forward and now a time to pause? Cell Stem Cell *15*, 535–536.

Le Gurun, S., Martin, D., Formenton, A., Maechler, P., Caille, D., Waeber, G., Meda, P., and Haefliger, J.A. (2003). Connexin-36 contributes to control function of insulin-producing cells. J. Biol. Chem. *278*, 37690–37697.

Levin, M. (2007). Gap junctional communication in morphogenesis. Prog. Biophys. Mol. Biol. *94*, 186–206.

Lim, P.K., Bliss, S.A., Patel, S.A., Taborga, M., Dave, M.A., Gregory, L.A., Greco, S.J., Bryan, M., Patel, P.S., and Rameshwar, P. (2011). Gap junction-mediated import of microRNA from bone marrow stromal cells can elicit cell cycle quiescence in breast cancer cells. Cancer Res. *71*, 1550–1560.

Nishii, K., Shibata, Y., and Kobayashi, Y. (2014). Connexin mutant embryonic stem cells and human diseases. World J. Stem Cells *6*, 571–578.

Nlend, R.N., Michon, L., Bavamian, S., Boucard, N., Caille, D., Cancela, J., Charollais, A., Charpantier, E., Klee, P., Peyrou, M., et al. (2006). Connexin36 and pancreatic beta-cell functions. Arch. Physiol. Biochem. *112*, 74–81.

Nostro, M.C., Sarangi, F., Yang, C., Holland, A., Elefanty, A.G., Stanley, E.G., Greiner, D.L., and Keller, G. (2015). Efficient generation of NKX6-1+ pancreatic progenitors from multiple human pluripotent stem cell lines. Stem Cell Reports *4*, 591–604.

Opsahl, H., and Rivedal, E. (2000). Quantitative determination of gap junction intercellular

communication by scrape loading and image analysis. Cell Adhes. Commun. *7*, 367–375.

Pagliuca, F.W., Millman, J.R., Gürtler, M., Segel, M., Van Dervort, A., Ryu, J.H., Peterson, Q.P., Greiner, D., and Melton, D.A. (2014). Generation of functional human pancreatic β cells in vitro. Cell *159*, 428–439.

Peng, Q., Yue, C., Chen, A.C.H., Lee, K.C., Fong, S.W., Yeung, W.S.B., and Lee, Y.L. (2019). Connexin 43 is involved in early differentiation of human embryonic stem cells. Differentiation *105*, 33–44.

Rezania, A., Bruin, J.E., Arora, P., Rubin, A., Batushansky, I., Asadi, A., O'Dwyer, S., Quiskamp, N., Mojibian, M., Albrecht, T., et al. (2014). Reversal of diabetes with insulin-producing cells derived in vitro from human pluripotent stem cells. Nat. Biotechnol. *32*, 1121–1133.

Rezania, A., Bruin, J.E., Riedel, M.J., Mojibian, M., Asadi, A., Xu, J., Gauvin, R., Narayan, K., Karanu, F., O'Neil, J.J., et al. (2012). Maturation of human embryonic stem cell-derived pancreatic progenitors into functional islets capable of treating pre-existing diabetes in mice. Diabetes *61*, 2016–2029.

Rezania, A., Riedel, M.J., Wideman, R.D., Karanu, F., Ao, Z., Warnock, G.L., and Kieffer, T.J. (2011). Production of functional glucagon-secreting α-cells from human embryonic stem cells. Diabetes *60*, 239–247.

Russ, H.A., Parent, A.V., Ringler, J.J., Hennings, T.G., Nair, G.G., Shveygert, M., Guo, T., Puri, S., Haataja, L., Cirulli, V., et al. (2015). Controlled induction of human pancreatic progenitors produces functional beta-like cells in vitro. EMBO J. *34*, 1759–1772.

Serre-Beinier, V., Bosco, D., Zulianello, L., Charollais, A., Caille, D., Charpantier, E., Gauthier, B.R., Diaferia, G.R., Giepmans, B.N., Lupi, R., et al. (2009). Cx36 makes channels coupling human pancreatic β-cells, and correlates with insulin expression. Hum. Mol. Genet. *18*, 428–439.

Serre-Beinier, V., Mas, C., Calabrese, A., Caton, D., Bauquis, J., Caille, D., Charollais, A., Cirulli, V., and Meda, P. (2002). Connexins and secretion. Biol. Cell *94*, 477–492.

Scherer, S.S., Xu, Y.-T., Messing, A., Willecke, K., Fischbeck, K.H., and Jeng, L.J.B. (2005). Transgenic expression of human Connexin32 in myelinating schwann cells prevents demyelination in connexin32-null mice. J. Neurosci. *25*, 1550–1559.

Sambathkumar, R., Migliorini, A., and Nostro, M.C. (2018). Pluripotent stem cell-derived pancreatic progenitors and β-Like cells for Type 1 diabetes treatment. Physiology (Bethesda) *33*, 394–402.

Sneddon, J.B., Tang, Q., Stock, P., Bluestone, J.A., Roy, S., Desai, T., and Hebrok, M. (2018). Stem cell therapies for treating diabetes: progress and remaining challenges. Cell Stem Cell *22*, 810–823.

Sozen, B., Can, A., and Demir, N. (2014). Cell fate regulation during preimplantation development: a view of adhesion-linked molecular interactions. Dev. Biol. *395*, 73–83.

Söhl, G., and Willecke, K. (2004). Gap junctions and the connexin protein family. Cardiovasc. Res. *62*, 228–232.

Tang, C., Weissman, I.L., and Drukker, M. (2013). Immunogenicity of in vitro maintained and matured populations: potential barriers to engraftment of human pluripotent stem cell derivatives. Methods Mol. Biol. *1029*, 17–31.

Ware, C.B., Nelson, A.M., Mecham, B., Hesson, J., Zhou, W., Jonlin, E.C., Jimenez-Caliani, A.J., Deng, X., Cavanaugh, C., Cook, S., et al. (2014). Derivation of naive human embryonic stem cells. Proc. Natl. Acad. Sci. U S A *111*, 4484–4489.

Wei, C.J., Xu, X., and Lo, C.W. (2004). Connexins and cell signaling in development and disease. Annu. Rev. Cell Dev. Biol. *20*, 811–838.

Wang, Y., and Belousov, A.B. (2011). Deletion of neuronal gap junction protein connexin 36 impairs hippocampal LTP. Neurosci. Lett. *502*, 30–32.

Weng, S., Lauven, M., Schaefer, T., Polontchouk, L., Grover, R., and Dhein, S. (2002). Pharmacological modification of gap junction coupling by an antiarrhythmic peptide via protein kinase C activation. FASEB J. *16*, 1114–1146.

Willecke, K., Eiberger, J., Degen, J., Eckardt, D., Romualdi, A., Güldenagel, M., Deutsch, U., and Söhl, G. (2002). Structural and functional diversity of connexin genes in the mouse and human genome. Biol. Chem. *383*, 725–737.

Wörsdörfer, P., Bosen, F., Gebhardt, M., Russ, N., Zimmermann, K., Komla Kessie, D., Sekaran, T., Egert, A., Ergün, S., Schorle, H., et al. (2017). Abrogation of gap junctional communication in ES cells results in a disruption of primitive endoderm formation in embryoid bodies. Stem Cells *35*, 859–871.

Xu, X., Browning, V.L., and Odorico, J.S. (2011). Activin, BMP and FGF pathways cooperate to promote endoderm and pancreatic lineage cell differentiation from human embryonic stem cells. Mech. Dev. *128*, 412–427.

Yamada, A., Futagi, M., Fukumoto, E., Saito, K., Yoshizaki, K., Ishikawa, M., Arakaki, M., Hino, R., Sugawara, Y., Ishikawa, M., et al. (2016). Connexin 43 is necessary for salivary gland branching morphogenesis and FGF10-induced ERK1/2 phosphorylation. J. Biol. Chem. *291*, 904–912.

Yirme, G., Amit, M., Laevsky, I., Osenberg, S., and Itskovitz-Eldor, J. (2008). Establishing a dynamic process for the formation, propagation, and differentiation of human embryoid bodies. Stem Cells Dev. *17*, 1227–1241.

Zhu, S., Russ, H.A., Wang, X., Zhang, M., Ma, T., Xu, T., Tang, S., Hebrok, M., and Ding, S. (2016). Human pancreatic beta-like cells converted from fibroblasts. Nat. Commun. *7*, 10080.

Supplemental Information

Connexin 43 Functions as a Positive Regulator

of Stem Cell Differentiation into Definitive

Endoderm and Pancreatic Progenitors

Wendy Yang, Paul D. Lampe, Patricia Kensel-Hammes, Jennifer Hesson, Carol B. Ware, Laura Crisa, and Vincenzo Cirulli

METHODS

Culture of human embryonic stem cells human (hESCs).

H1, H1-OCT4 (WiCell, Madison, WI) and Elf-1 hESC lines (Ware et al., 2014) were passaged using dispase (1U/ml), and maintained as primed in feeder-free cultures under hypoxic conditions (5% C02, 5%O2, and 90% N2) on Matrigel-coated dishes (BD Biosciences), using TeSR medium (StemCell Technologies, Vancouver, BC, V6A 1B6, Canada) supplemented with 1x PenStrep, NEAA, sodium pyruvate, and Glutamine, as described (Ware et al., 2014). Experiments of hESC directed differentiation were carried out following slight modifications of published protocols (D'Amour et a., 2006; Xu et al., 2011; Rezania et al. 2014; Pagliuca et al., 2014; Russ et al., 2015; Jennings et al., 2015; Nostro et al., 2015; Sambathkumar et al., 2018; Sneddon et al., 2018). Briefly, on day 1 70% sub-confluent hESC monolayers received RPMI medium without serum containing Activin A (100 ng/mL) and Wnt3a (30 ng/mL). On day 2 and 3 medium was replaced with RPMI 0.2% KSR, Activin A (100 ng/mL), followed by RPMI 2% KSR, supplemented with KGF (50 ng/mL) on days 4, 5 and 6. Subsequently, on days 7, 8 and 9 the differentiation medium consisted in DMEM 1% B27, Cyclopamine (0.25 mM), TTNBP (3 nM), Noggin (50 ng/mL), followed by DMEM 1% B27, Noggin (50 ng/mL), KGF (50 ng/mL), EGF (50 ng/mL) on days 10, 11, and 12. Finally, on days 13-16 cultures received DMEM 1% B27, without any additional factors. Activation of Cx43 by the AAP10 peptide [H-Gly-Ala-Gly-Hyp-Pro-Tyr-CONH(2)] (Genscript) in differentiating hESC cultures was conducted from day 1 to day 3 (AAP10 Stop @ DE), or from day 1 until the end of the differentiation protocol (AAP10 Throughout) using a concentration of 400nM.

For siRNA experiments, undifferentiated hESCs monolayers were transfected with 50nM of a control non-targeting siRNA (Qiagen, Allstars negative control

siRNA) or a pool of CX43-specific siRNAs (Darmacon ON-TARGETplus SMART pool) using GenMute transfection reagent, as per manufacturer's instructions. On the day following siRNA transfection, hESCs were differentiated toward DE as described above, and analyzed for the expression of the DE markers E-cadherin and CXCR4 by flow cytometry at day 2 and day 3 post-differentiation. siRNA-mediated down-regulation of Cx43 was routinely validated by Western Blotting and found to result in >70% reduction of the protein in all experiments (not shown).

Carboxyfluorescein (CF) transfer assay

To monitor GJ-mediated CF transfer between cells in contact, we used a slight modification of the method previously described by Opsahl and Rivedal (Opsahl and Rivedal, 2000). Briefly, hESC monolayers at the DE stage of differentiation were first washed with plain RPMI without proteins, and then in HBSS containing Carboxyfluorescein (1:10 dilution of a saturated stock) and Rhodamine Dextran (0.05%) in the presence or absence of AAP10 peptide (400 nM). In some experiments, to assess the specificity of dye uptake through GJ, DE cultures were pretreated with Carbenoxolone (CBX) for 30 minutes prior to the scrape loading assay. Scratches across hESC colonies were then done using sterile pipette tips. After 5 minutes incubation at 37 °C, the HBSS containing the dyes was washed away three times, and replaced with medium without phenol red. DIC and fluorescent images were then collected at 5 and 15 minutes using an Olympus inverted microscope, equipped with an epifluorescence X-Cite Series 120Q UV lamp, and a SpotInsight 5MP Color Camera (Pacific Microsystems LLC).

RNA extraction and Quantitative RT-PCR (qPCR)

RNA was isolated from hESC cultures at each step of differentiation using Aurum™ Total RNA Mini Kit (Bio-Rad) according to the manufacturer's instructions, and retrotranscribed into cDNA using the Superscript III (Invitrogen), and primers listed in Table I; q-PCR reactions was performed in triplicate using the Sybr Green kit (Bio-Rad), and data analysed using Bio-Rad CFX Manager software.

Western Blots

Total protein extracts from hESC cultures at each step of differentiation were prepared in lysis buffer (10mM Tris-HCl pH7.8; 150mM NaCl; 1mM EDTA; 200 um sodium orthovanadate and protease inhibitor cocktail tablet (IP 1x, MALT, 1 mM DTT, 1mM PMSF), separated on an SDS-PAGE gel (30 μg/lane), and transferred onto a nitrocellulose membrane as previously described (Diaferia et al., 2013; Yebra et al., 2003; Jimenez-Caliani et al., 2017). Membranes were then washed in PBST (1 × PBS, 0.1% Tween pH 7.4), blocked with 3% non-fat milk for 1h, incubated in primary antibodies (Table II) diluted in 1% BSA in PBST overnight at 4°C, then washed with PBST and incubated with HRP-conjugated secondary antibody for 1h at room °t. After washing, chemoluminescence signal was detected using the ECL™ Western Blotting Analysis System (Amersham/GE Healthcare).

Flow cytometry

hESC cultures at each step of differentiation were harvested using a non-enzymatic cell dissociation medium (Sigma), and incubated in FACS buffer (HBSS 0.2% BSA) with either FITC-conjugated anti E-cadherin (clone 67A4,

Biolegend) or PE-conjugated anti-CXCR4 (clone 12G5, Biolegend) antibodies (Table III). Samples were then analysed at a FACSCalibur flow cytometer using the FlowJo software (FlowJo, LLC, V8.8.6).

Immunofluorescence and morphometric analysis

H1 hESC lines (WiCell, Madison, WI) were cultured on glass coverslips up to subconfluency and then differentiated as described above. Cells at each differentiation stage were fixed in 2% paraformaldehyde, and processed for immunofluorescence staining as described (Yebra et al., 2013; Diaferia et al., 2013). Briefly, after permeabilization with 0.05% Triton X100, coverslips with cells were incubated for 10 minutes with blocking buffer containing 50mM glycine, 2% donkey serum and 1% BSA in PBS. Next, combinations of primary antibodies (Table II) diluted in PBS (0.2% donkey serum, 0.1% BSA) were applied and incubated either overnight at 4 C, or for 1 hour at room temperature. After three washes in PBS (0.2% donkey serum, 0.1% BSA), fluorophore-conjugated secondary antibodies (Fab)[2] fractions; Jackson Immunoresearch Labs) were applied, and incubated for 45 minutes at room temperature. Coverslips were then washed and mounted for viewing at a Nikon Eclipse *90i* microscope, equipped with an epifluorescence X-Cite Series 120Q UV lamp. Images were then acquired using 10X, 20X, or 40X Nikon objectives, using the NIS-Elements AR-3.2 software (Nikon). Immunostaining of cryosections from hESC-derived embryoid bodies was conducted following virtually the same procedure.

STATISTICS

Were applicable, statistical significance of differences in data values was validated by analysis of variance (ANOVA), followed by Bonferroni's Multiple

Comparison Test, or by two tailed Student's *t* test, using the Prism-4 statistical package (Graph Pad Software, San Diego, CA), with significance limit set at p<0.05.

Table I: qPCR Primers

Target	Forward	Reverse
18s	CCTGCGGCTTAATTTGACTC	GACAAATCGCTCCACCAACT
Cx26	CAAACCGCCCAGAGTAAAGA	CTTTCCAATGCTGGTGGAGT
Cx32	TGAGACCATAGGGGACCTGT	TCATCACCCCACACACTCTC
Cx36	GCAGCAGCACTCCACTATGA	AAGCAAAGACTGGGGGTACA
Cx43	GTGCCTGAACTTGCCTTTTC	CCCTCCAGCAGTTGAGTAGG
CxCR4	CCGTGGCAAACTGGTACTTT	GACGCCAACATAGACCACCT
Ecad	GAACGCATTGCCACATACAC	ATTCGGGCTTGTTGTCATTC
FoxA2	ATTGCTGGTCGTTTGTTGTG	TACGTGTTCATGCCGTTCAT
Glucagon	AAGTTCCCAAAGAGGGCTTG	AGCTGCCTTGTACCAGCATT
GSC	GAACCTCTTCCAGGAGACCA	CGTTCTCCGACTCCTCTGAT
Hnf1b	CAACCAGACTCACAGCCTGA	TGCCATGGTGACTGATTGTT
Hnf4a	GAATGCGACTCTCCAAAACC	TGAGGTTGGTGCCTTCTGAT
Hnf6	AACCCTGGAGCAAACTCAAA	GAGTTCGACGCTGGACATCT
Insulin	CTACCTAGTGTGCGGGGAAC	GCTGGTAGAGGGAGCAGATG
MafA	GCGGAGAACGGTGATTTCTA	AGGAAAGGGAGGCTGAGAAG
Nanog	GCCGAAGAATAGCAATGGTG	ACTGGATGTTCTGGGTCTGG
Ncad	AGCCAACCTTAACTGAGGAGT	GGCAAGTTGATTGGAGGGAT
Ngn3	CCCTCTACTCCCCAGTCTCC	CCTTACCCTTAGCACCCACA
Nkx2.2	TCTACGACAGCAGCGACAAC	TTGTCATTGTCCGGTGACTC
Nkx6.1	CCCGGGCTCTACTTCAGC	TCTTCCCGTCTTTGTCCAAC
Oct4	TGCTCCAGCTTCTCCTTCTC	CGCCGTATGAGTTCTGTGG
Pdx1	CCTTTCCCATGGATGAAGTC	TTCAACATGACAGCCAGCTC
Sox17	AGCAGAATCCAGACCTGCAC	TTGTAGTTGGGGTGGTCCTG

Table II: Unconjugated antibodies

Antigen	Host	Source	Cat #
Cx36	Rabbit	U.S. Biological	C7855-14
Cx43 373	Rabbit	Paul Lampe	n.a.
Cx43 CT1	Mouse	Paul Lampe	n.a.
Cx43 NT1	Mouse	Paul Lampe	n.a.
Cx43 IF1	Mouse	Paul Lampe	n.a.
Hnf3β/FoxA2	Goat	R&D Systems	AF2400
p44/42 MAPK (ERK1/2)	Rabbit	Cell Signaling Technology Inc	#4695
p44/42 MAPK (ERK1/2)	Rabbit	Cell Signaling Technology Inc	#9101S
Sox17	Goat	R&D Systems	AF1924
α-Tubulin	Mouse	ABCAM	AB7291
β-catenin	Mouse	BD Transduction Labs	610153
Cx43 IF1	Mouse	Paul Lampe	n.a.
E-cadherin	Mouse	BD Transduction Labs	610182
FoxA2	Goat	R&D Systems	AF2400
Nanog	Rabbit	Stemgent	09-0020
Oct 4	Rabbit	Stemgent	09-0023
PCNA	Mouse	Santa Cruz	sc-56
Pdx1	Goat	BCBC	n.a.
pH3	Rabbit	MILLIPORE	06-570
Sox17	Goat	R&D Systems	AF1924
Sox9	Rabbit	Millipore	AB5535

Table III: Fluorophore-conjugated antibodies

Antigen	Fluorophore	Vendor	Cat #
CD184 (CXCR4)	PE	Biolegend	306506
CD324 (Ecad)	PerCP/Cy5.5	Biolegend	324114
Hnf3b/FoxA2	Alexa Fluor ®488	R&D Systems	IC2400G
Sox17	PE	R&D Systems	IC19241P